Thermochimica Acta, 95 (1985) 179–200
Elsevier Science Publishers B.V., Amsterdam – Printed in The Netherlands

KINETICS OF DISSOCIATION OF HYDRATED CERIUM(III) SULFATE, NITRATE AND OXALATE IN AIR

AHMED M. GADALLA
Chemical Engineering Department, Texas A&M University, College Station, TX 77843 (U.S.A.)
(Received 20 May 1985)

ABSTRACT

Simultaneous thermal analysis curves and X-ray examination were used to determine the intermediate steps for the dissociation of hydrated cerium(III) sulfate and to confirm those for the dissociation of hydrated cerium(III) nitrate and oxalate. Thermogravimetric methods were applied for these steps to determine the operating mechanisms and kinetic parameters. These methods were assessed in view of the present results. Techniques to treat similar results were recommended to overcome the difficulties encountered during this study, such as the variation of activation energies and pre-exponential factors with temperature for the same mechanism as well as the change of the mechanism with temperature. Methods for differentiation between the deduced mechanisms to conclude the operating mechanism are discussed. Techniques to deal with mechanisms having low activation energies or existing over wide temperature ranges are still needed.

INTRODUCTION

Classical chemical reaction kinetics have been mainly concerned with homogeneous reactions and terms such as reaction order or frequency factor are generally meaningless when applied to heterogeneous reactions. In limited cases, only when the reaction order is 0, 1/2, 2/3 or 1, the equations have theoretical significance. This paper reviews methods for dealing with heterogeneous reactions, which are accompanied by change in weight, when heated with a constant heating rate. The use of thermogravimetric curves was emphasized since they give the most reliable results for the operating mechanisms, activation energies and pre-exponential factors. Even when an overlap occurs in such curves, the initial part may frequently yield sufficient information for the first reaction (or mechanism) whereas the tail end of the overlap may be used for the second reaction (or mechanism).

One of the objectives of this study is to establish the intermediate compounds and steps for dissociating hydrated cerium(III) sulfate using combined thermal analysis.

0040-6031/85/$03.30

The second objective is to assess the various techniques for studying heterogeneous reactions when applied to the established intermediate steps for dissociating hydrated cerium(III) sulfate, nitrate and oxalate. The present author has already established the intermediate steps for the last two salts.

The third objective is to recommend the best technique to treat similar results confidently and to overcome difficulties such as: (a) having different possible mechanisms with completely different kinetic parameters for the same reaction over the same temperature range; (b) having more than one operating mechanism depending on the working temperature; or (c) having wide ranges for the activation energy and the pre-exponential factor for the same mechanism.

PREVIOUS WORK

Hydrated cerium(III) sulfate

Udupa [1] stated that the decomposition of $Ce_2(SO_4)_3 \cdot 14H_2O$ in air is similar to that in argon and occurs over three distinct stages.

$$50\text{–}190°C: Ce_2(SO_4)_3 \cdot 14H_2O = Ce_2(SO_4)_3 \cdot 5H_2O + 9H_2O \quad (1)$$

$$210\text{–}300°C: Ce_2(SO_4)_3 \cdot 5H_2O = Ce_2(SO_4)_3 + 5H_2O \quad (2)$$

$$700\text{–}920°C: Ce_2(SO_4)_3 = 2CeO_2 + 2SO_3 + SO_2 \quad (3)$$

The activation energy for the third reaction was reported to be 47 kcal mol^{-1} using the Coats and Redfern [2] equation (see below).

Hydrated cerium(III) nitrate

El-Adham and Gadalla [3] studied the dissociation of $Ce(NO_3)_3 \cdot 6H_2O$ in air. Below 100°C the salt dissociates giving liquid water which dissolves the lower hydrate forming a transparent, colourless solution, thus elevating the boiling point. During evaporation of the water, a yellow dihydrate starts dissociating.

$$Ce(NO_3)_3 \cdot 6H_2O = \text{solution} = Ce(NO_3)_3 \cdot 2H_2O + 4H_2O \quad (4)$$

$$Ce(NO_3)_3 \cdot 2H_2O = Ce(NO_3)_3 + 2H_2O \quad (5)$$

The anhydrous nitrate dissociates with the evolution of brownish fumes of nitrogen oxides and oxidation of cerium to cerium(IV) oxide.

$$Ce(NO_3)_3 = CeO_2 + N_2O_5 + NO_2 \quad (6)$$

Hydrated cerium(III) oxalate

El-Adham and Gadalla [3] studied the dissociation of the heptahydrate in air and found the following steps to occur.

$$Ce(C_2O_4)_3 \cdot 7H_2O = Ce(C_2O_4)_3 \cdot 3H_2O + 4H_2O \quad (7)$$

$$Ce(C_2O_4)_3 \cdot 3H_2O = Ce(C_2O_4)_3 + 3H_2O \quad (8)$$

Bad resolution was obtained for the dissociation of the anhydrous salt to the cerium(IV) oxide but DTA showed the overlapping of an exothermic peak and two endothermic peaks. The two endothermic peaks may correspond to dissociation of the anhydrous oxalate to carbonate followed by decomposition to the oxide. The exothermic peak may be due to oxidation of the CO, evolved during the first step, and/or oxidation of Ce_2O_3 produced as an intermediated crystallization of an initially amorphous product.

THEORY

Due to the limited information on heterogeneous reactions most research workers adopted the equations established for homogeneous reactions and considered the reaction rate to be proportional to the nth power of the unreacted material, α represents the fraction reacted.

$$d\alpha/dt = k(1-\alpha)^n \quad (9)$$

In heterogeneous reactions, there is a reaction interface between the reacting phases and after forming stable nuclei which grow above the critical size, some of (or all) the following steps take place: mass transfer of reactants to the interface, reaction at the boundary, mass transfer of the products away from the interface, or grain boundary movement. The reaction at the phase boundary liberates or absorbs heat changing its temperature and accordingly heat transfer to or from the boundary may limit the rate of the process. The slowest of the above-mentioned steps will be the rate-determining step.

Astonishingly, the results obtained for heterogeneous reactions fit the reaction order equation well in spite of the fact that eqn. (9) is correct only for homogeneous reactions and in spite of the fact that the physical meaning of the reaction order (n) no longer holds. The equations developed can have theoretical significance only in those cases where the value of n is 0, 1/2, 2/3, or 1. These values correspond to the following rate-controlling step:

(1) $n = 0$, one-dimensional movement of phase boundary or zero reaction order (as a burning fuse);

(2) $n = 1/2$, two-dimensional movement of phase boundary (as an expanding or contracting cylinder);

(3) $n = 2/3$, three-dimensional movement of phase boundary (as an expanding or contracting sphere).

The rate constant, k, was considered to be related to temperature by the Arrhenius equation

$$k = A\mathrm{e}^{-E/RT} \tag{10}$$

This equation is only correct for activated processes but cannot be used for nonactivated processes, such as heat transfer. In the case of gaseous homogeneous reactions, the frequency factor (A) is proportional to the number of successful collisions of the reacting molecules. According to the kinetic theory of gases, A is proportional to $T^{1/2}$ and, according to statistical mechanics, it is proportional to T. In the case of combustion of coal particles, which is a diffusion-controlled process, the activation energy is zero and the pre-exponential term is proportional to $T^{1.75}$. In heterogeneous solid-state reactions, A cannot be called the frequency factor; it is just a pre-exponential term which can be considered constant if the change occurs over an extremely narrow temperature range, or if the change requires a large activation energy. In the latter case, the strong exponential function masks the effect of the weaker functions $T^{1/2}$, T or $T^{1.75}$.

The rate equation can be written for isothermal processes in the general form

$$\mathrm{d}\alpha/\mathrm{d}t = k\mathrm{f}(\alpha) \tag{11}$$

While House [4] used a semi-logarithmic curve fit to relate α and T, Šesták and Berggren [5] proposed that $\mathrm{f}(\alpha) = \alpha^m(1-\alpha)^n[-\ln(1-\alpha)^q]$. Expressions of $\mathrm{f}(\alpha)$ for the various rate-controlling steps are shown in Table 1.

For a constant heating rate, $\beta = \mathrm{d}T/\mathrm{d}t$, and for activated processes, eqns. (10) and (11) can be combined to give

$$\beta[\mathrm{d}\alpha/\mathrm{d}T] = A\mathrm{f}(\alpha)\mathrm{e}^{-E/RT} \tag{12}$$

$$\ln[\beta\mathrm{d}\alpha/\mathrm{d}T] = \ln[A\mathrm{f}(\alpha)] - E/RT \tag{13}$$

If $\mathrm{f}(\alpha)$ is known, Sharp et al. 's method [6,7] can be used, i.e., by plotting the left-hand side against $1/T$, a straight line is obtained from which E and A can be determined. On the other hand, if $\mathrm{f}(\alpha)$ is unknown, Caroll and Manche [8] showed that the activation energy can be calculated by plotting $\ln(\beta\mathrm{d}\alpha/\mathrm{d}T)$ vs. $1/T$ at a fixed value of α obtained from a series of TG curves at different heating rates.

The reaction mechanism may be determined by comparing the experimental data for a single TG curve with the various kinetic equations (Table 1) using eqn. (12).

The above-mentioned methods depend on determining the first derivative and are thus known as differential methods. Integral methods can be deduced by rearranging eqn. (12) as follows

$$\mathrm{d}\alpha/\mathrm{f}(\alpha) = [A/\beta]\ \exp(-E/RT)\mathrm{d}T \tag{14}$$

TABLE 1

Kinetics of heterogeneous solid-state reactions

Rate-determining mechanism	Symbol	$f(\alpha)$	$g(\alpha)=\int_0^\alpha d\alpha/f(\alpha)$
Nucleation and nuclei growth			
(1) *Random nucleation* with one nucleus in each individual particle (Mampel unimolecular law)	F_1	$1-\alpha$	$-\ln(1-\alpha)$
(2) *Avrami–Erofeev nuclei growth*			
Two-dimensional growth	A_2	$2(1-\alpha)\times[-\ln(1-\alpha)]^{1/2}$	$-[\ln(1-\alpha)]^{1/2}$
Three-dimensional growth	A_3	$3(1-\alpha)\times[-\ln(1-\alpha)]^{2/3}$	$-[\ln(1-\alpha)]^{1/3}$
Prout–Tompkins branching nuclei	A_1	$\alpha(1-\alpha)$	$\ln \alpha/(1-\alpha)$
Diffusion			
Parabolic law (one-dimensional transport process)	D_1	α^{-1}	$\alpha^2/2$
Valensi two-dimensional diffusion (cylinder with no volume change)	D_2	$[-\ln(1-\alpha)]^{-1}$	$(1-\alpha)\ln(1-\alpha)+\alpha$
Three-dimensional diffusion spherical symmetry (Jander mech.)	D_3	$(1-\alpha)^{1/3}\times[(1-\alpha)^{-1/3}-1]^{-1}$	$1.5[1-(1-\alpha)^{1/3}]^2$
Three-dimensional diffusion Brounshtein–Ginstling mech.	D_4	$[(1-\alpha)^{-1/3}-1]^{-1}$	$1.5[1-2\alpha/3-(1-\alpha)^{2/3}]$
Phase boundary movement			
One-dimensional (zero order)	R_1	Const.	α
Two-dimensional (cylindrical symmetry)	R_2	$(1-\alpha)^{1/2}$	$2[1-(1-\alpha)^{1/2}]$
Three-dimensional (spherical symmetry)	R_3	$(1-\alpha)^{2/3}$	$3[1-(1-\alpha)^{1/3}]$
Power law		$(1-\alpha)^n$	$[1-(1-\alpha)^{1-n}]/(1-n)$

Integrating eqn. (14) and replacing $\int d\alpha/f(\alpha)$ by the function $g(\alpha)$, which is shown for various mechanisms in Table 1, the equation for a TG curve can be obtained

$$g(\alpha) = [A/\beta] \int \exp(-E/RT)dT \tag{15}$$

To find the values of the right-hand side, earlier workers [9–11] expressed the exponential part (roughly) in terms of the maximum reaction rate temperature (T_m). These methods give accurate results only if the reactions proceed over a narrow temperature range (between 0.9 T_m and 1.1 T_m).

According to Van Krevelen et al. [9]

$$\log(\alpha) = \log[A/\beta]\left[(0.368/T_m)^{E/RT_m}(E/RT_m + 1)^{-1}\right] + (E/RT_m + 1)\log T \tag{16}$$

While equations of Horowitz and Metzger [10] are proposed for particular cases, the equations proposed by Reich [11] can be used for results obtained at two different heating rates.

$$E = \frac{2.303R\log\dfrac{\beta_2}{\beta_1}\left[\dfrac{T_1}{T_2}\right]^2}{\dfrac{1}{T_1} - \dfrac{1}{T_2}} \tag{17}$$

Accurate results can also be obtained using Coats and Redfern's approximation [2]. Although their initial equation was derived assuming the power law mechanism, it could be modified and generalized to suit the heterogeneous reactions.

$$\log\frac{g(\alpha)}{T^2} = \log\frac{AR}{E\beta} - \frac{E}{2.3RT} \tag{18}$$

Accordingly, $\log[g(\alpha)/T^2]$ is to be calculated for all possible mechanisms and the best straight line determines the operating mechanism; E and A can be calculated from the slope and the intercept.

Another approach to overcome the tediousness of the trial and error, is to integrate eqn. (14) and write the result in the form

$$g(\alpha) = [AE/R\beta]p(x) \tag{19}$$

where $p(x)$ is a function depending on both temperature and activation energy and has been tabulated by various authors. To facilitate calculations, Šatava and Škvàra [12] plotted $p(x)$ vs. T for various activation energies and tabulated the values of $g(\alpha)$ for various mechanisms based on exact numerical integration. They demonstrated the following equation.

$$\log g(\alpha) - \log p(x) = \text{constant} = \log(AE/R\beta) \tag{20}$$

Values of $\log g(\alpha)$ are plotted against T for all possible mechanisms and are superimposed over a $\log p(x)$ chart so that the temperature scales coincide. The curves are then shifted along this ordinate until one of the $\log g(\alpha)$ curves fits one of the $\log p(x)$ curves. The activation energy can be read and the equation governing the kinetics can be established. Equation (20) can then be used to determine A.

It should be mentioned that Kissinger [13] was one of the earlier workers who used DTA to calculate the activation energy. Based on the assumption that the peak temperature of DTA (T_p) is close to the temperature of

maximum rate (T_m), Kissinger derived eqn. (21) assuming a power law kinetic equation (eqn. 9).

$$\ln A = \ln(E/R) - \ln\left(T_p^2/\beta\right) + E/RT_p \quad (21)$$

Plotting $\ln[T_p^2/\beta]$ vs. $1/T_p$ will give a straight line of slope E/R. Ravindran et al. [14] proved that this equation gives accurate results only if T_p is close to T_m. Accordingly, the present author used Kissinger's equation with T_m (read from DTG curves) instead of T_p.

It should be noted that difference differential methods are not popular because of the magnification of experimental scatter and, accordingly, they were not reviewed.

EXPERIMENTAL TECHNIQUES

Pure hydrated compounds supplied by Prolabo were heated in the Derivatograph to obtain DTA, TG and DTG curves simultaneously. Calcined alumina was selected as a reference material and other parameters are indicated in Table 2.

Supplemented by X-ray diffraction techniques, the thermal curves (Fig. 1) were used to determine the dissociation steps and compositions of the intermediate compounds formed during the dissociation of hydrated cerium(III) sulfate. For the other salts (Figs. 2 and 3) the intermediate steps were found to agree with the previous work mentioned earlier.

RESULTS AND DISCUSSION

Dissociation steps of cerium(III) sulfate octahydrate

After complete dissociation, a constant weight was achieved (Fig. 1). The residue was examined by X-ray diffraction and was found to be CeO_2. From the total weight loss the number of molecules of water of hydration was

TABLE 2

Operating conditions

Salt	Mass (mg)	Heating rates (K min^{-1})	Atm.	Crucible
$Ce_2(SO_4)_3 \cdot 8H_2O$	500	6, 10, 13	Air	Pt
$Ce(NO_3)_3 \cdot 6H_2O$	700	5, 7, 10	Air	Pt
$Ce_2(C_2O_4)_3 \cdot 7H_2O$	300	6, 10, 13	Air	Pt

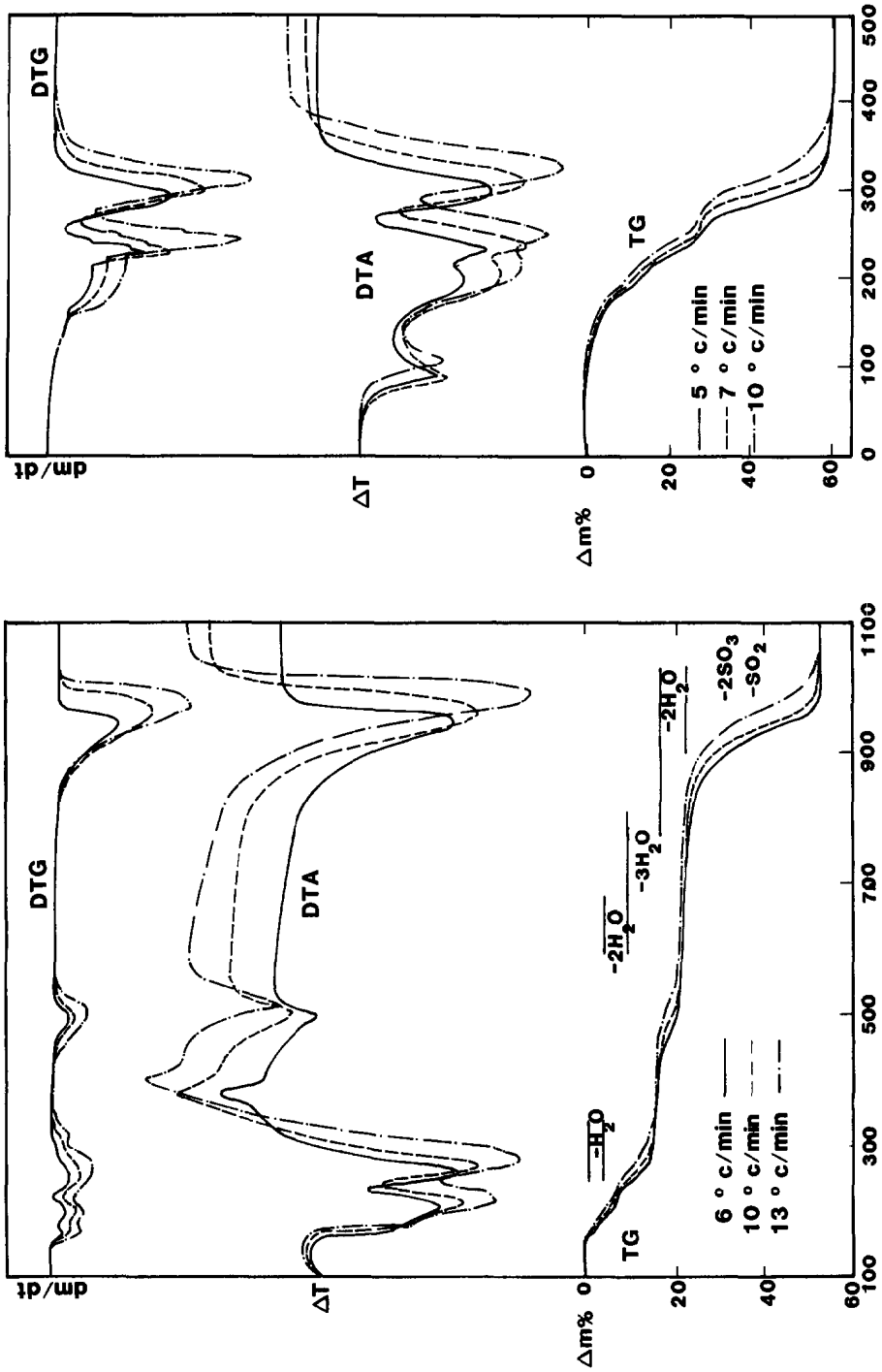

Fig. 1. Thermal curves of $Ce_2(SO_4)_3 \cdot 8H_2O$.

Fig. 2. Thermal curves of $Ce(NO_3)_3 \cdot 6H_2O$.

calculated and the composition was found to be $Ce_2(SO_4)_3 \cdot 8H_2O$ and not $Ce_2(SO_4)_3 \cdot 14H_2O$ as stated by Udupa [1].

The beginning and end of any change can be estimated from DTG curves and the exact temperature at which the maximum rate occurs, T_m, can be determined. TG curves were used to calculate the intermediate compositions reached corresponding to any change after excluding the initial weight loss which is due to moisture content.

From Fig. 1 it could be concluded that the dissociation steps are

$$Ce_2(SO_4)_3 \cdot 8H_2O = Ce_2(SO_4)_3 \cdot 7H_2O + H_2O_{(g)}$$

$$Ce_2(SO_4)_3 \cdot 7H_2O = Ce_2(SO_4)_3 \cdot 5H_2O + 2H_2O_{(g)}$$

$$Ce_2(SO_4)_3 \cdot 5H_2O = \alpha\text{-}Ce_2(SO_4)_3 \cdot 2H_2O + 3H_2O_{(g)}$$

Peaks on DTA which are not accompanied by weight changes represent either a phase change (allotropic transformation or a change from a metastable to a stable phase) or a fast solid-state reaction not accompanied by gas absorption or evolution. Between 340 and 420°C an exothermic peak was observed which was not accompanied by any change in weight. Table 3 shows the X-ray pattern for the material before and after this peak indicating a slight change in the *d* spacings with the same chemical composition. Accordingly, a phase change was assumed to occur

$$\alpha\text{-}Ce_2(SO_4)_3 \cdot 2H_2O = \beta\text{-}Ce_2(SO_4)_3 \cdot 2H_2O$$

At higher temperatures, depending on the heating rate, the dihydrate dissociates to CeO_2.

$$\beta\text{-}Ce_2(SO_4)_3 \cdot 2H_2O = Ce_2(SO_4)_3 + 2H_2O$$

and

$$Ce_2(SO_4)_3 = 2CeO_2 + 2SO_3 + SO_2$$

The formation of CeO_2 as a final product was confirmed by X-ray analysis. Oxidation of cerium to the tetravalent state may be due to reduction of SO_3 to SO_2 as indicated above or, more probably, due to oxidation of the fresh, active crystallites of Ce_2O_3 formed from dissociation of cerium(III) sulfate according to the reactions

$$Ce_2(SO_4)_3 = Ce_2O_3 + 3SO_3$$

and

$$Ce_2O_3 + 1/2O_2 = 2CeO_2$$

Transition temperatures obtained here are reproducible if stagnant air is used. Other temperatures will be obtained for the same powder, in the same

TABLE 3

X-ray diffraction pattern for α- and β-$Ce_2(SO_4)_3 \cdot 2H_2O$

α-form		β-form	
d (Å)	I/I_0 (%)	d (Å)	I/I_0 (%)
		4.92	25
4.64	100	4.64	100
4.43	45	4.43	40
3.42	45	3.42	60
3.21	75	3.21	90
3.14	25	3.14	35
2.97	35	2.97	40
2.90	25	2.90	25
2.82	45	2.82	50
2.728	20	2.728	35
2.688	45	2.688	40
2.600	25	2.600	35
2.319	25		
2.100	35	2.100	35
2.046	35		
2.006	35	2.006	35
1.832	25		
		1.560	35
		1.380	25
		1.315	25
		1.220	15
		1.085	25
		1.042	25

crucible at the same heating rate, if the partial pressure of H_2O, SO_2, SO_3, O_2 or nitrogen oxides changes.

Dissociation mechanisms and kinetic parameters

As explained previously, to obtain correct results using Kissinger's technique, DTG curves and not DTA were used and temperatures corresponding to the maximum rate were used instead of peak temperatures on DTA. For each step, $\ln(T^2/\beta)$ was plotted against $1/T$ (eqn. 21); a typical straight line is shown in Fig. 4. The slope of the straight line is E/R. The results obtained for the various dissociation steps for the three hydrates are given in Tables 4–6.

Reich's equation (17) was used to give the activation energy for each of the two heating rates. Average values for each step were calculated and are also given in Tables 4–6.

It should be noted that the above-mentioned methods are based on the assumption that the corresponding reactions proceed over narrow tempera-

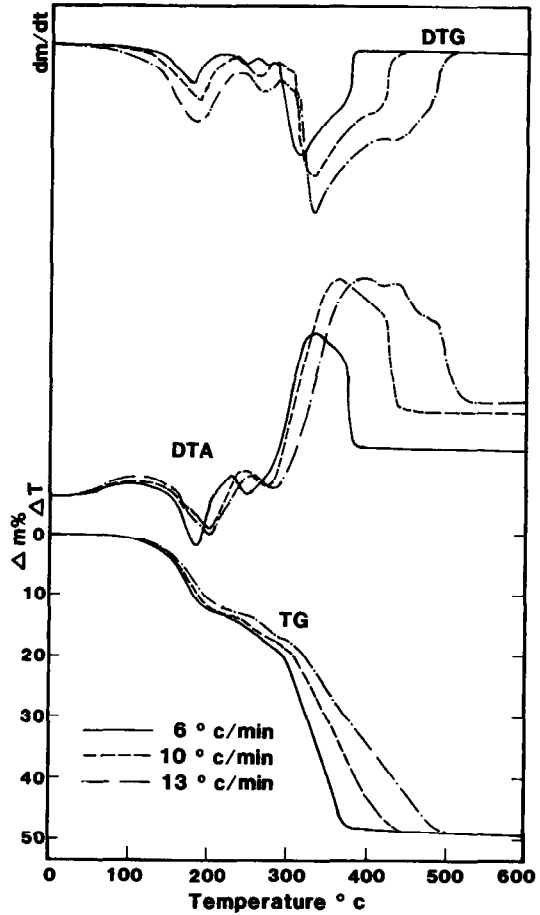

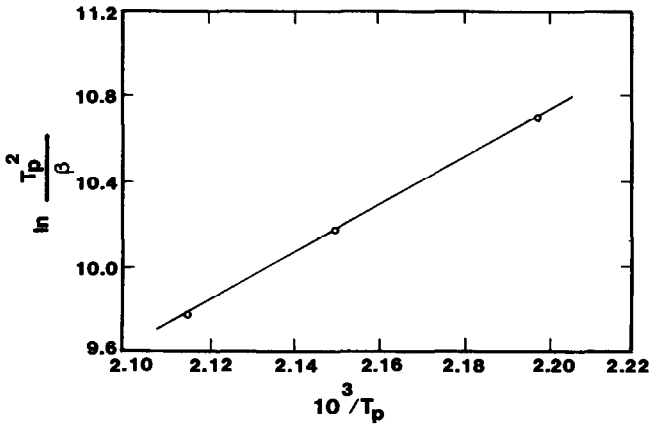

Fig. 3. Thermal curves of $Ce_2(C_2O_4)_3 \cdot 7H_2O$.

Fig. 4. Determination of the activation energy for the reaction $Ce_2(C_2O_4)_3 \cdot 7H_2O = Ce_2(C_2O_4)_3 \cdot 3H_2O + 4H_2O_{(g)}$ using Kissinger's method.

TABLE 4

Possible controlling processes and kinetic parameters for dissociation of hydrated cerium(III) sulfate

Reaction	DTG		TG					
	Kissinger E (kcal mol^{-1})	Reich E_{av} (kcal mol^{-1})	Carroll and Manche E_{av} (kcal mol^{-1})	Coats and Redfern			Šatava and Škvàra	
				Mech.	E (kcal mol^{-1})	A (min^{-1})	Mech.	E (kcal mol^{-1})
$Ce_2(SO_4)_3 \cdot 8H_2O =$	30	30	41				A_2	20
$Ce_2(SO_4)_3 \cdot 7H_2O$				A_3	12	$9.3(10)^4$	or A_3	15
$+ H_2O$				or R_2	29	$6.1(10)^{13}$	or R_2	30 [a]
				or $\underline{R}_3$	32	$1.6(10)^{15}$	or $\underline{R}_3$	35 [a]
				or D_3	65	$1.4(10)^{31}$	or D_3	70
$Ce_2(SO_4)_3 \cdot 7H_2O =$				A_2	48	$1.3(10)^{22}$		
$Ce_2(SO_4)_3 \cdot 5H_2O$				or $\underline{A}_3$	33	$5.7(10)^{14}$	$\underline{A}_3$	25
$+ 2H_2O$	26	26	21	followed by			followed by	
				A_2	17	$2.2(10)^4$		
				or $\underline{A}_3$	11	$1.5(10)^7$	$\underline{A}_3$	10
				or R_2	21	$1.6(10)^9$		
				or R_3	26	$1.9(10)^{11}$		
$Ce_2(SO_4)_3 \cdot 5H_2O =$				$\underline{A}_2$	28	$1.4(10)^{11}$	$\underline{A}_2$ [b]	23
$Ce_2(SO_4)_3 \cdot 2H_2O$				or A_3	18	$6.5(10)^6$	or A_3 [b]	15
$+ 3H_2O$				or F_1	58	$8.0(10)^{23}$		
				or R_2	55	$7.7(10)^{22}$		
				or R_3	56	$1.6(10)^{23}$	or R_3	50
				or D_1	108	$6.2(10)^{44}$		
				or D_2	112	$1.3(10)^{46}$		
				or D_3	114	$8.6(10)^{46}$		
				or D_4	112	$8.5(10)^{45}$		
	24 [c]	23 [c]	6	followed by			followed by	
				$\underline{A}_2$	4	1.48	$\underline{A}_2$ [d]	5
				or A_3	1.7	$9.6(10)^{-2}$		
				or F_1	10	$1.3(10)^3$	or F_1 [d]	10
				or R_1	0.1	$1.1(10)^{-3}$		
				or R_2	3.2	$6.8(10)^{-1}$		
				or R_3	4.8	5.3		
				or D_1	2.5	$8.5(10)^{-2}$		
				or D_2	5.4	3.8		
				or D_3	11.9	$1.9(10)^3$		
				or D_4	7.3	1.2(10)		
$Ce_2(SO_4)_3 \cdot 2H_2O =$				A_2	21	$1.9(10)^5$	A_2	20
$Ce_2(SO_4)_3 + 2H_2O$				or A_3	13	$5.1(10)^2$	or A_3	12
				or F_1	46	$4.1(10)^{12}$	or F_1	40 [e]
				or R_1	39	$3.1(10)^{10}$	or R_1	35
				or R_2	42	$3.3(10)^{11}$		

TABLE 4 (continued)

Reaction	DTG		TG						
	Kissinger E (kcal mol^{-1})	Reich E_{av} (kcal mol^{-1})	Carroll and Manche E_{av} (kcal mol^{-1})	Coats and Redfern			Šatava and Škvàra		
				Mech.	E (kcal mol^{-1})	A (min^{-1})	Mech.	E (kcal mol^{-1})	
				or R_3	43	$7.5(10)^{11}$	or R_3	41 [e]	
				or D_1	81	$3.3(10)^{22}$			
				or D_2	85	$6.3(10)^{23}$			
				or D_3	89	$5.5(10)^{24}$	or D_3	85	
				or D_4	86	$5.8(10)^{23}$			
	41	41	19	followed by			followed by		
				A_2	4	$2.6(10)^{-1}$	A_2	5	
				or A_3	1.3	$1.9(10)^{-2}$			
				or F_1	10	$8.7(10)^{-1}$	or F_1	10	
				or R_3	5	$8.6(10)^{10}$	or R_3	5	
$Ce_2(SO_4)_3 =$				R_2	64	$3.5(10)^{11}$	R_2	55	
$2CeO_2 + 2SO_3 + SO_2$	56 [c]	57 [c]	46	or R_3	70	$4.8(10)^{11}$			

[a] R_2 and R_3 are possible but R_3 gives a slightly better fit.
[b] A_2 and A_3 are possible but A_2 gives a slightly better fit.
[c] This reaction occurs over a wide range of temperature (wider than the range 0.9 T_m–1.1 T_m which gives accurate results).
[d] A_2 and F_1 are possible but A_2 gives a slightly better fit.
[e] F_1 and R_3 are possible but R_3 gives a slightly better fit.

ture ranges. Unfortunately, dissociation of $Ce_2(SO_4)_3 \cdot 5H_2O$ to the dihydrate, dissociation of $Ce_2(SO_4)_3$ to CeO_2, dissociation of $Ce(NO_3)_3$ to CeO_2 and dissociation of $Ce_2(C_2O_4)_3 \cdot 7H_2O$ to the dihydrate were found to exist over temperature ranges wider than the range 0.9 T_m–1.1 T_m. Accordingly, values of activation energies for these reactions are not expected to be accurate (compare these values with those obtained using other techniques).

For each step, curves showing α vs. T were also constructed for the three heating rates using the equation $\alpha = (m_0 - m_t)/(m_0 - m_v)$. Fixed values of α were selected and the slopes of the best straight lines, obtained by plotting $\beta d\alpha/dT$ vs. $1/T$ on semilog paper, were used to calculate the activation energies using eqn. (13). Average values are listed in Tables 4–6 under the heading "Carroll and Manche".

It should be noted that the above three techniques determine the activation energy without knowing the mechanism. To determine, for each step, the rate-determining mechanism and the corresponding kinetic parameters, the following two techniques were used.

TABLE 5

Possible controlling processes and kinetic parameters for dissociation of hydrated cerium(III) nitrate

Reaction	DTG		TG					
	Kissinger E (kcal mol^{-1})	Reich E_{av} (kcal mol^{-1})	Carroll and Manche E_{av} (kcal mol^{-1})	Coats and Redfern			Šatava and Škvàra	
				Mech.	E (kcal mol^{-1})	A (min^{-1})	Mech.	E (kcal mol^{-1})
$Ce(NO_3)_3 \cdot 6H_2O$ = solution								
Solution = $Ce(NO_3)_3 \cdot 2H_2O_{(s)} + 4H_2O_{(g)}$	18	19	25	R_1 or $\underline{D_1}$	10 22	$4.6(10)^3_9$ $\underline{1.6(10)}$	R_1 $\underline{D_1}$	10 20
$Ce(NO_3)_3 \cdot 2H_2O$ = $Ce(NO_3)_3 + 2H_2O$	16	16	32	R_2 or $\underline{R_3}$ [a] or D_3	32 35 71	$1.2(10)^{13}_{14}$ $\underline{3.0(10)}$ $6.5(10)^{29}$	R_2 or $\underline{R_3}$ [a] or D_3	30 35 70
$Ce(NO_3)_3$ = $CeO_2 + N_2O_5 + NO_2$				$\underline{F_1}$ [b] or A_2 or A_3 or R_2 or R_3 or D_2 or D_3	45 21 14 41 42 82 87	$\underline{8.7(10)}^{16}$ $3.2(10)^7$ $1.8(10)^4$ $1.9(10)^{15}$ $6.5(10)^{15}$ $6.2(10)^{30}$ $3.0(10)^{32}$	$\underline{F_1}$ or A_2 or R_2 or R_3 or D_3	40 [b] 25 40 40 80
	18 [c]	16 [c]	12	followed by $\underline{F_1}$ [d] or A_2 or A_3 or R_2 or R_3 or D_2 or D_3	12 5 2 6 7 15	$\underline{4.7(10)}^3$ 2.9 $1.7(10)^{-1}$ $1.3(10)^1$ 8.2 $1.2(10)^4$	followed by $\underline{F_1}$	15

[a] R_2 and R_3 are possible but R_3 gives a slightly better fit.

[b] F_1 gives a curve passing through more points.

[c] This reaction occurs over a range of temperature wider than the range 0.9 T_m–1.1 T_m which gives accurate results.

[d] It was difficult to select the governing mechanism using this method. Best fit was determined by Šatava and Škvàra.

Coats and Redfern's equation

For each step, TG curves were used to calculate $\log[g(\alpha)/T^2]$ for each possible controlling mechanism (Table 1). These were plotted against $1/T$. Such curves are shown in Fig. 5 for reaction (7) when a heating rate of 6 K min^{-1} was used. According to eqn. (18) the best straight line fitting the points determines the mechanism and fixed E and A. One of the difficulties

TABLE 6

Possible controlling processes and kinetic parameters for dissociation of hydrated cerium(III) oxalate

Reaction	DTG		TG					
	Kissinger E (kcal mol^{-1})	Reich E_{av} (kcal mol^{-1})	Carroll and Manche E_{av} (kcal mol^{-1})	Coats and Redfern			Šatava and Škvàra	
				Mech.	E (kcal mol^{-1})	A (min^{-1})	Mech.	E (kcal mol^{-1})
$Ce_2(C_2O_4)_3 \cdot 7H_2O =$				R_3	14	$1.2(10)^6$	R_3	15
$Ce_2(C_2O_4)_3 \cdot 3H_2O$	21 [a]	22 [a]	15	or D_3	29	$1.4(10)^{13}$	or D_3	30
$+4H_2O$				or A_3	4	6.1(10)		
$Ce_2(C_2O_4)_3 \cdot 3H_2O =$				or R_2	22	$2.6(10)^8$		
$3H_2O + Ce_2(C_2O_4)_3$	22	22	22	or R_3	24 [b]	$2.5(10)^9$	R_3	25
				or D_3	50	$5.9(10)^{19}$		
$Ce_2(C_2O_4)_3 + 2O_2 =$				A_2	22	$2.2(10)^7$	A_2	20
$2CeO_2 + 6CO_2$				or A_3	14	$1.5(10)^4$	or A_3	10
				or R_1	45	$4.9(10)^{15}$	or R_1	40
(a) $Ce_2(C_2O_4)_3 =$				or F_1	47	$3.5(10)^{16}$	or F_1	40
$Ce_2(CO_3)_3 + 3CO$			12	or R_2	46	$1.3(10)^{16}$		
				or R_3	46	$1.8(10)^{16}$	or R_3	40
$3CO + 3/2O_2 =$				or D_2	93	$1.5(10)^{33}$		
$3CO_2$				or D_3	94	$1.8(10)^{33}$		
				or D_4	93	$5.5(10)^{32}$		
	13	12		followed by			followed by	
(b) $Ce_2(CO_3)_3 =$				A_2	12	$1.8(10)^3$	A_2	10
$Ce_2O_3 + 3CO_2$				or A_3	7	$2.0(10)^1$	or A_3	10
				or R_2	17	$7.7(10)^4$		
$Ce_2O_3 + 1/2O_2 =$			7	or R_3	20	$1.0(10)^7$	or R_3	20
$2CeO_2$				or D_3	42	$1.8(10)^{13}$	or D_3	40
				or D_4	34	$1.7(10)^{10}$		

[a] This reaction occurs over a range of temperature wider than the range 0.9 T_m–1.1 T_m which gives accurate results.

[b] R_2 and R_3 are possible but R_3 was selected in view of the results obtained by Šatava and Škvàra.

observed is that more than one straight line can fit the results (Fig. 5). Straight lines with high correlation coefficients and low standard deviation were selected to represent the possible controlling mechanisms. The corresponding kinetic parameters were calculated and are shown in Tables 4–6 under the heading "Coats and Redfern", separated by "or". On the other hand, if it was difficult to find a straight line fitting all the experimental points, more than one mechanism operates and two straight lines were selected. Figure 6 was constructed for the dissociation of $Ce_2(C_2O_4)_3$ to CeO_2 using a heating rate of 6 K min^{-1} and is shown to demonstrate this

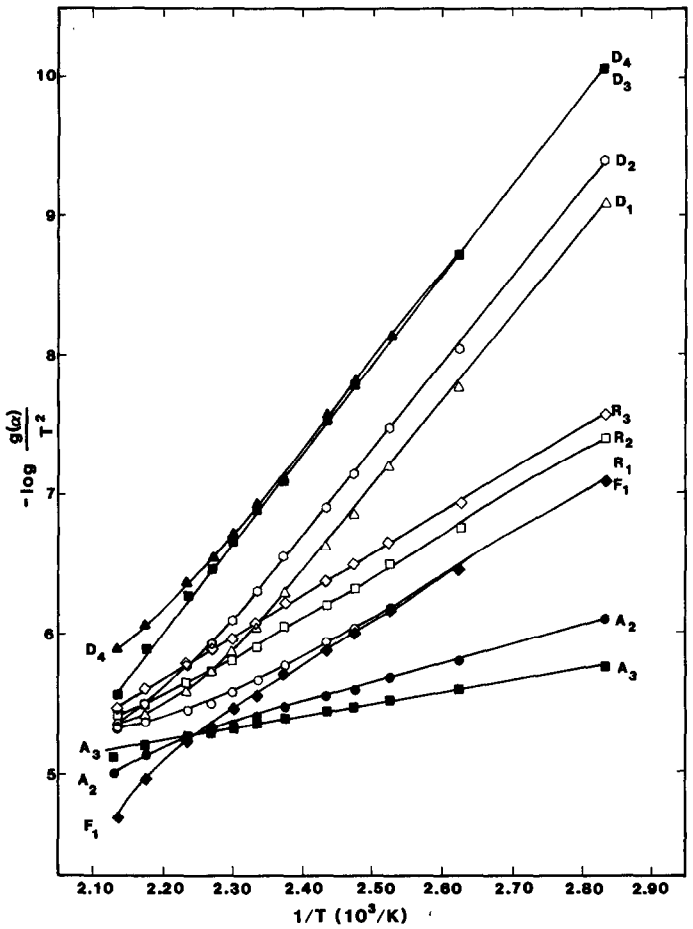

Fig. 5. Variation of $\log[g(\alpha)/T^2]$ with $1/T$ for various mechanisms for reaction (7) using a heating rate of 6 K min^{-1}.

difficulty. The set of parameters which may operate at low temperatures was calculated and is indicated first, in Tables 4–6, followed by those corresponding to possible high-temperature mechanisms.

Šatava and Škvàra's technique

A chart showing the variation of log p(x) vs. T was constructed and a set of curves obtained for various activation energies. Values of log g(α) for the possible controlling mechanisms (Table 1) were calculated and plotted against T on transparent paper using the same scales used for constructing p(x) curves. Figure 7 shows such curves obtained for reaction (7) using a rate of 6°C min^{-1}. Šatava and Škvàra's technique was used and the values of activation energy read from the chart are given in Tables 4–6. When more than one g(α) curve coincided with p(x) curves, the corresponding mechanisms and their activation energies are presented in the Tables separated by "or". On the other hand, if no curve for g(α) coincides completely with any

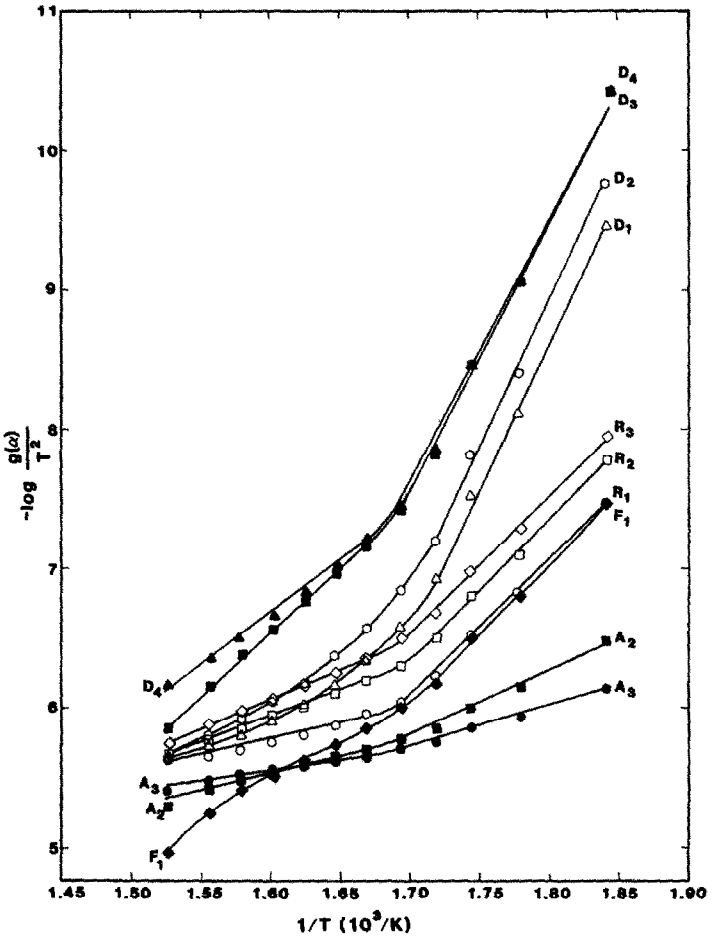

Fig. 6. Variation of $\log[g(\alpha)/T^2]$ with $1/T$ for various mechanisms for the dissociation of $Ce_2(C_2O_4)_3$ to CeO_2 using a heating rate of 6 K min^{-1}.

p(x) curve this indicates that the process is governed by more than one mechanism. Values obtained at lower temperatures are reported first followed by those corresponding to the higher temperature mechanism(s). Since the values of E obtained for the possible mechanisms were close to those calculated by Coats and Redfern's method, and since values of A can be calculated using the same equation, the expected values of A will be near the values indicated under the heading "Coats and Redfern" in Tables 4–6.

It was noted that when Coats and Redfern's or Šatava and Škvàra's techniques were applied for the same reaction, the activation energy and the pre-exponential factor decreased with increasing heating rate. The values indicated in Tables 4–6 represent the average values (arithmetic) obtained using the rates investigated (Table 2). It should be noted that Ninan and Nair [15] studied the effect of the heating rate and the mass of the specimen

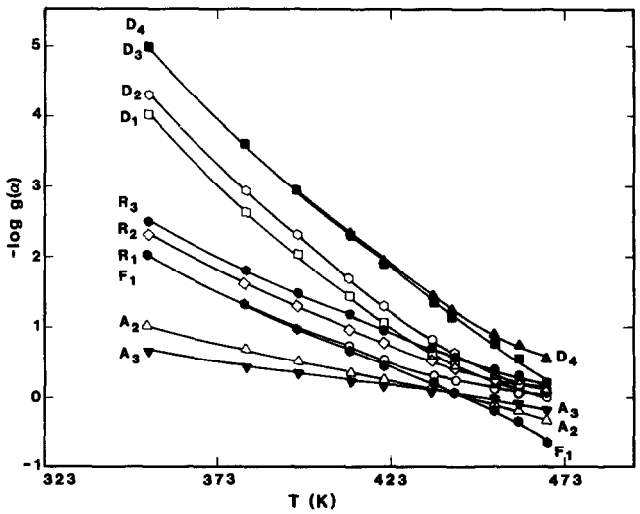

Fig. 7. Variation of log g(α) with temperature for various mechanisms for reaction (7) using a rate of 6 K min^{-1}.

on the kinetic parameters in another system. It seems that the corresponding decrease of the pre-exponential factor tries to compensate the change in the activation energy with increased heat flux to give slight changes in the rate constant.

To explain why the results over a limited temperature range can fit more than one mechanism (Fig. 5), reference should be made to Table 1. It is obvious that $\log g(\alpha)_{D_3} = 2\log g(\alpha)_{R_3} + \text{const.}$, and $\log g(\alpha)_{A_3} = n \log g(\alpha)_{A_2}$. This indicates that both R_3 and D_3 will give straight lines with different slopes. Accordingly, the activation energy for D_3 will be double that calculated for R_3. This conclusion is in harmony with results shown in Tables 4–6. Similarly, if one of Avrami–Erofeev's mechanisms operate, A_2 and A_3 will give straight lines with different slopes.

Moreover, Criado and Morales [16] reported that D_2 and R_2 on one hand and D_4 and R_3 on the other hand are related by the equations

$$\ln[(1-\alpha)\ln(1-\alpha)+\alpha] = 1.89 \ln[1-(1-\alpha)^{1/2}] + 0.4$$

$$\ln[1-2\alpha/3-(1-\alpha)^{2/3}] = 1.84 \ln[1-(1-\alpha)^{1/3}] - 0.46$$

The above equations indicate that differentiation between D_3, D_4 and R_3 or D_2 and R_2 is difficult and give relations between the various slopes (the activation energy corresponding to various mechanisms). To differentiate between these mechanisms Criado and Morales [16] recommended using isothermal techniques in addition to TG curves.

Another difficulty, which was also observed in the present work and was reported by Ball and Casson [17], is that the values of g(α) for nucleation

mechanisms are much smaller than those for others which also fit well (see Figs. 5 and 6). This may lead to wrong conclusions that these mechanisms are the controlling steps.

To overcome the above difficulties, values obtained using techniques based on Kissinger, Reich, or Carroll and Manche's equations for determining the average activation energies were used as a guide to differentiate between the best possible mechanisms. The operating mechanism and the corresponding kinetic parameters, thus selected for each step, were underlined (Tables 4–6).

It is evident from the tables that methods based on temperature corresponding to the maximum rate could not differentiate between overlapping mechanisms or reactions and give only one value, which was considered here to be an average value.

It is to be remembered that in all the methods investigated the activation energy and pre-exponential factors were considered constant. On the other hand, if we consider the results obtained for the dissociation of $Ce_2(SO_4)_3 \cdot 5H_2O$ to the dihydrate, the dissociation of β-$Ce_2(SO_4)_3 \cdot 2H_2O$ to the anhydrous sulfate and the dissociation of $Ce(NO_3)_3$ to CeO_2, it is evident that in each case the same mechanism operates but the values of E and A vary considerably. It could be concluded that these values vary uniformly over the operating temperatures. This conclusion implies that the theoretical part of this paper will be correct only if the changes in these values are small and average values are used in the derived equations. Accordingly, the Reich and Kissinger methods are not suitable for reactions occurring over a wide temperature range or when activation energies and pre-exponential factors vary over wide ranges. Similarly, Carroll and Manche's method assumes that the same mechanism operates over the range of temperatures at which the same value of α is reached with constant activation energy and pre-exponential factor. In view of the above results, this may not be true. Moreover, the results are very sensitive to a slight variation in the slope, $d\alpha/dT$, and are not reliable, but these values are just sufficient to select the operating mechanism using the Coats and Redfern technique or Šatava and Škvàra's technique.

The number of possible mechanisms obtained using Šatava and Škvàra's technique is much less than the number obtained by Coats and Redfern's technique. The latter technique determines the transition temperatures between consecutive mechanisms more easily and sharply. Only in cases when the possible mechanisms have similar or very low activation energies should the two techniques be followed to select the best fit. It should also be noted that with low activation energy the exponential part in eqn. (10) could not mask the variation of the pre-exponential factor with temperature. A new set of equations should be deduced to account for the variation of A as a function of temperature.

CONCLUSIONS

(1) Hydrated cerium(III) sulfate was found to dissociate to the heptahydrate which dissociates to the pentahydrate then to the dihydrate. The latter phase was found to exist in two allotropic forms with a transition temperature lying in the range 340–420°C. The two forms were X-rayed and their diffraction patterns were included. At higher temperatures, depending on the heating rate, the anhydrous salt is formed and dissociates to CeO_2 which was confirmed by X-ray analysis. The oxidation of cerium to the tetravalent state indicates that either SO_3 and SO_2 are produced as by-products or the fresh active crystallites of Ce_2O_3 oxidize immediately in air.

(2) Although various steps were found to be governed completely by single mechanisms and each mechanism has a fixed activation energy and pre-exponential factor, dissociation of $Ce_2(SO_4)_3 \cdot 5H_2O$ to the dihydrate, dissociation of $Ce_2(SO_4)_3 \cdot 2H_2O$ to anhydrous sulfate and dissociation of $Ce(NO_3)_2$ to CeO_2 took place by single mechanisms. For each reaction the activation energy and pre-exponential factor vary over wide ranges and decrease with increasing temperature. These results imply that the techniques based on the assumption that these values are constants will yield inaccurate results in similar cases. Accordingly, methods based on the maximum rate temperature, T_m, such as Reich's technique or the modified Kissinger's technique, gave inaccurate results for the above-mentioned reactions. Moreover, these techniques were also based on the assumption that the reactions proceed over narrow temperature ranges. Reactions which took place over a temperature range wider than the range 0.9 T_m–1.1 T_m, such as dissociation of $Ce_2(SO_4)_3 \cdot 5H_2O$ to the dihydrate, dissociation of $Ce_2(SO_4)_3$ to CeO_2, dissociation of $Ce(NO_3)_3$ to CeO_2 and dissociation of $Ce_2(C_2O_4)_3 \cdot 7H_2O$ to the dihydrate, gave inaccurate results.

(3) Carroll and Manche's technique was found to be very sensitive to slight variations in the slope, $d\alpha/dT$, and is not reliable. In addition to this, it assumes that the same mechanism operates, with the same kinetic parameters, over the range of temperatures at which a same degree of decomposition is reached.

(4) While methods based on the maximum rate temperature could not differentiate between overlapping mechanisms or reactions, methods based on the modified equation of Coats and Redfern or on Šatava and Škvàra's technique can differentiate between the operating mechanisms, can overcome the changes in kinetic parameters with temperature and can fix them more accurately. The disadvantage of these techniques is that more than one possible mechanism with different kinetic parameters may be produced. The Coats and Redfern mechanism gave more possibilities and the reasons for this were discussed. To overcome these difficulties it is recommended that the activation energy is determined roughly using Carroll and Manche's technique for various heating rates and this value used to select the operating

mechanism from those obtained using the above techniques. When possible mechanisms have similar activation energies both techniques (Coats and Redfern on one hand and Šatava and Škvàra on the other hand) are needed to select the best fit.

(5) The above method was used to determine the apparent operating mechanism and kinetic parameters for the various steps in air for the specimen amounts indicated. Since the activation energies and the pre-exponential factors were found to decrease with increasing heating rate, the values reported here are only valid for the range of heating rates indicated in Table 2. For other heating rates the effect of the change in the pre-exponential factor does not compensate the effect of changes in the activation energy and different rate constant will be obtained.

(6) All the techniques, developed for studying kinetics using constant heating rates, are unreliable if the activation energy is low or if the mechanism operates over a wide temperature range. In such a case the pre-exponential factor is temperature-sensitive and a new set of equations is required to describe the possible operating mechanisms.

NOTATION

A	frequency factor (pre-exponential factor for Arrhenius equation)
d	interplanar distances in crystals
E	activation energy (kcal mol^{-1})
I/I_0	percentage relative intensity for the peaks of the X-ray diffraction pattern
k	rate constant
m	mass at the beginning of step
m_v	mass at the end of step
m_t	mass at the temperature T
n	apparant reaction rate
R	universal gas constant
t	time
T	absolute temperature
α	decomposed fraction $= (m_0 - m_t)/(m_0 - m_v)$
β	heating rate, dT/dt

ACKNOWLEDGEMENT

The author wishes to acknowledge the effort made by Dr. Ahmed Nasr-El-Din for running the derivatograph to obtain the thermal curves.

REFERENCES

1 M.R. Udupa, Thermochim. Acta, 57 (1982) 337.
2 A.W. Coats and J.P. Redfern, Nature (London), 201 (1964) 68.
3 K.A. El-Adham and A.M. Gadalla, Interceram, 26 (1977) 223.
4 J.E. House, Thermochim. Acta, 42 (1980) 369.
5 J. Šesták, and G. Berggren, Thermochim. Acta, 3 (1971) 1.
6 J.H. Sharp, G.W. Brindley and B.N. Achar, J. Am. Ceram. Soc., 49 (1966) 379.
7 J.H. Sharp and S.A. Wentworth, Anal. Chem., 41 (1969) 2060.
8 B. Carroll and E.P. Manche, Thermochim. Acta, 3 (1972) 449.
9 D.W. Van Krevelen, C. Van Heerden and F.J. Huntjens, Fuel, 30 (1951) 253.
10 H.H. Horowitz and G. Metzger, Anal. Chem., 35 (1963) 1464.
11 L. Reich, J. Polym. Sci., 2 (1964) 621.
12 Šatava and F. Škvàra, J. Am. Ceram. Soc., 52 (1969) 591.
13 H.E. Kissinger, J. Res. Natl. Bur. Stand., 57 (1956) 712.
14 P.V. Ranvindran, T.P. Radha Krishnan and A.K. Sundaram, Reaction Kinetics by TG and DTA Methods, Bhabha Atomic Research Center, Bombay, India, 1977, p. 927.
15 K.N. Ninan and C.G.R. Nair, Thermochim. Acta, 30 (1979) 25.
16 J.M. Criado and J. Morales, Thermochim. Acta, 19 (1977) 305.
17 M.C. Ball and M.J. Casson, Thermochim. Acta, 27 (1978) 387.